Thermochimica Acta, 215 (1993) 65–82
Elsevier Science Publishers B.V., Amsterdam

The application of non-isothermal methods of kinetic analysis to the decomposition of calcium hydroxide

Dun Chen, Xiang Gao and David Dollimore

Department of Chemistry and College of Pharmacy, The University of Toledo, Toledo, OH 43606 (USA)

(Received 10 June 1992)

Abstract

In this paper, the kinetic analysis of the thermogravimetric curves for the decomposition process of calcium hydroxide (under dry nitrogen atmosphere) is performed. Various forms of non-isothermal methods of analysis for determining the kinetic parameters are used. The calcium hydroxide samples were a commercial sample and samples prepared by reacting calcium nitrate with sodium hydroxide solutions at concentrations of 1 and 0.1 M. All the methods show that in the heating rate ranges 5–40°C min^{-1}, the most probable reaction mechanism for commercial calcium hydroxide is the Avrami–Erofeev equation (A) with $n = 1.5$ (i.e. A1.5), for calcium hydroxide prepared from 1 M solutions is A2 and for calcium hydroxide prepared from 0.1 M solutions is A1.5. The data also show that the distribution of particles and the change of the particle size are factors which affect the reaction mechanism.

INTRODUCTION

The decomposition process of calcium hydroxide is

$$Ca(OH)_2 \rightarrow CaO + H_2O$$

in the range 300–550°C. It has been investigated many times since the late 19th Century [1–6]. The reported information deals with the dissociation temperature and the heat of the reaction. Halstead and Moore [6] studied the equilibrium pressure of water above CaO and $Ca(OH)_2$ in the range 300–510°C and found the enthalpy ΔH of the reaction to be 104.18 kJ mol^{-1}. The published studies [7, 8] on the kinetics of the $Ca(OH)_2$–CaO–H_2O system show a great variation in the values obtained. The probable reason for this is the difference in the degree of crystallinity of the calcium hydroxide used in the various reports.

In order to have a systematic kinetic analysis of the decomposition of calcium hydroxide, different forms of calcium hydroxide should be

Correspondence to: D. Chen, Department of Chemistry and College of Pharmacy, The University of Toledo, Toledo, OH 43606, USA.

prepared by changing the formation conditions. Both commercial calcium hydroxide and pure calcium hydroxide prepared by precipitation are used in this paper.

EXPERIMENTAL

Materials

The commercial analytical calcium hydroxide reagent used in this paper was from Mallinckodt.

Pure calcium hydroxide samples were prepared by mixing different concentrations of sodium hydroxide solution with calcium nitrate solution. The concentrations used were 1 and 0.1 M. CH1M means calcium hydroxide prepared from 1 M NaOH and 1 M $Ca(NO_3)_2$. CH01M means calcium hydroxide prepared from 0.1 M NaOH and 0.1 M $Ca(NO_3)_2$. Both NaOH and $Ca(NO_3)_2$ solutions were prepared from analytical sodium hydroxide and calcium nitrate solids. The precipitates were filtered under vacuum after mixing the appropriate solutions for 30 min, washed thoroughly twice with distilled water, twice with ethanol and once with acetone. The products were then dried in an oven at 110°C for 3 h. Samples were then stored in a desiccator.

Techniques

All the thermogravimetric (TG) and derivative thermogravimetric (DTG) experiments are carried out on the Du Pont 1090 thermal analyzer with a 951 TGA thermogravimetric analyzer. The heating rates used were 5, 10, 20 and 40°C min^{-1} under dry nitrogen atmosphere. The sample sizes were 13 ± 0.7 mg and everything else was normalized.

The raw data was transmitted from the RS-232C port of the DuPont 1090 to a connected computer and was then further analyzed.

The X-ray powder diffraction (XRD) patterns were obtained on a Scintag XDS-2000 unit with an accelerating voltage of 45 kV and a current of 40 mA. The half peak width was calculated by using the Pearson VII peak profiting program on the DMS software. The surface areas of samples were obtained by using the single-point surface area unit [9] and the scanning electron microscopy (SEM) was performed on a JEOL JSM 6100 at 15 kV.

THEORY

In the kinetic analysis, it was found convenient to express a reaction by using a certain function $f(\alpha)$ of the reaction extent α, where in TG

$$\alpha = (W_i - W)/(W_i - W_f)$$

TABLE 1

The common forms of $f(\alpha)$ and $G(\alpha)$

Mechanism	$G(\alpha)$	$f(\alpha)$
Acceleratory α–t *curve*		
P1 Power law	$\alpha^{1/4}$	$4\alpha^{3/4}$
	$\alpha^{1/3}$	$3\alpha^{2/3}$
	$\alpha^{1/2}$	$2\alpha^{1/2}$
	α	1
	$\alpha^{3/2}$	$(2/3)\alpha^{-1/2}$
E1 Exponential law	$\ln \alpha$	α
S-Shaped α–t *curve*		
A1.5 Avrami–Erofeev	$[-\ln(1-\alpha)]^{2/3}$	$1.5(1-\alpha)[-\ln(1-\alpha)]^{1/3}$
A2 Avrami–Erofeev	$[-\ln(1-\alpha)]^{1/2}$	$2(1-\alpha)[-\ln(1-\alpha)]^{1/2}$
A3 Avrami–Erofeev	$[-\ln(1-\alpha)]^{1/3}$	$3(1-\alpha)[-\ln(1-\alpha)]^{2/3}$
A4 Avrami–Erofeev	$[-\ln(1-\alpha)]^{1/4}$	$4(1-\alpha)[-\ln(1-\alpha)]^{3/4}$
B1 Prout–Tompkins	$\ln[\alpha/(1-\alpha)]$	$\alpha(1-\alpha)$
	$[-\ln(1-\alpha)]^2$	$0.5(1-\alpha)[-\ln(1-\alpha)]^{-1}$
	$[-\ln(1-\alpha)]^3$	$(1/3)(1-\alpha)[-\ln(1-\alpha)]^{-2}$
	$[-\ln(1-\alpha)]^4$	$(1/4)(1-\alpha)[-\ln(1-\alpha)]^{-3}$
Deceleratory α–t *curve*		
R2 Contracting surface	$1-(1-\alpha)^{1/2}$	$2(1-\alpha)^{1/2}$
R3 Contracting volume	$1-(1-\alpha)^{1/3}$	$3(1-\alpha)^{2/3}$
D1 1-D Diffusion	α^2	$1/2\alpha$
D2 2-D Diffusion	$(1-\alpha)\ln(1-\alpha)+\alpha$	$-[\ln(1-\alpha)]^{-1}$
D3 3-D Diffusion	$(1-(1-\alpha)^{1/3})^2$	$1.5[1-(1-\alpha)^{1/3}]^{-1}(1-\alpha)^{2/3}$
D4 Ginstling–Brouns	$(1-2\alpha/3)-(1-\alpha)^{2/3}$	$1.5[1-(1-\alpha)^{1/3}]^{-1}$
F1 First order	$-\ln(1-\alpha)$	$1-\alpha$
F2 Second order	$1/(1-\alpha)$	$(1-\alpha)^2$
F3 Third order	$[1/(1-\alpha)]^2$	$0.5(1-\alpha)^3$

where W is the weight or the wt.% of the sample at a certain time. W_i and W_f are the initial and final values for the reaction.

The most commonly used equation to describe the reaction rate is the differential form

$$d\alpha/dt = f(\alpha)k(T) \tag{1}$$

where $f(\alpha)$ is the function of α which represents the reaction mechanism. Table 1 shows a list of the most commonly used equations. $k(T)$ is the rate constant at the temperature T and it generally takes the Arrhenius equation form

$$k(T) = A\exp(-E/RT) \tag{2}$$

where A is the pre-exponential factor or frequency factor, E is the activation energy, R is the gas constant and T is the absolute temperature.

If we combine eqns. (2) and (1) and rearrange them, we obtain

$$d\alpha/f(\alpha) = A \exp(-E/RT)\, dT/\beta \quad (3)$$

where β is the heating rate, which is dT/dt. The integration of the right-hand side of eqn. (3) is impossible and many approximations [10–12] to this integration have been made. The one used here was proposed by Madhusudanan [12], i.e.

$$\ln[G(\alpha)/T^{1.921503}] = \ln(AE/\beta R) + 3.7720501 - 1.921503 \ln E - E/RT \quad (4)$$

where $G(\alpha)$ is the integral form of the reaction function. Various forms of $G(\alpha)$ are shown in Table 1.

Differential method

There are two kinetic methods used in this paper and both originate from combining eqns. (1) and (2) to give

$$d\alpha/dt = Af(\alpha) \exp(-E/RT) \quad (5)$$

In the first method (termed the single-heating-rate differential method) the logarithm of eqn. (5) is taken, to give

$$\ln[(d\alpha/dt)/f(\alpha)] = \ln A - E/RT$$

By feeding the experimental data from a single heating-rate curve, a plot of $\ln[(d\alpha/dt)/f(\alpha)]$ vs. $1/T$ is obtained by testing all the functions $f(\alpha)$ in Table 1. The linear regression can be calculated and then the activation energy E and the frequency factor A can be calculated from the slope and intercept of the regression line.

The second method was proposed by Friedman [13] and takes the form

$$\ln(d\alpha/dt)_i = \ln Af(\alpha_i) - E/RT_i$$

where the subscript i refers to the value of the variable at degree of conversion α_i from at least two or more experiments under different heating rates. Further, a plot of $\ln(d\alpha/dt)_i$ vs. $1/T_i$ is made by taking the experimental data directly from different heating-rate curves at the same α_i value. α_i takes values from 0.05 to 0.95 in steps of 0.05. The linear regression is then made to each α_i value and from the slope the activation energy, E can be calculated. In this paper, this method is called the Friedman method.

Integral method

From eqn. (4), the plot of $\ln[G(\alpha)/T^{1.921503}]$ vs. $1/T$ is made from a single experimental heating-rate curve and all the integral forms of the

function $G(\alpha)$ in Table 1 may be tested. The activation energy E and the frequency factor A is obtained from the slope and intercept of the linear fit line. This is the first integral method and is called the single-heating-rate integral method.

The second method in this paper is that proposed by Ozawa [14] and takes the form (after approximation as noted below)

$$-\log_{10}\beta_i - 0.4567E/RT_i = \text{constant}$$

where β_i and T_i are the heating rate and the absolute temperature for that heating rate with the same conversion α_i value. Therefore, at least two experiments with different heating rates must be made. The α_i values in this paper are chosen from between 0.05 and 0.95 in steps of 0.05. By plotting $\log_{10}\beta_i$ vs. $1/T_i$, the activation energy E is obtained from the slope of the best fitting line. This method is here called the Ozawa method.

RESULTS AND DISCUSSION

Theoretical calculation

In order to check the computer programs [15], a set of data was created from the theoretical calculation of the A1.5 mechanism with an activation energy $E = 120\,\text{kJ mol}^{-1}$ and a frequency factor $A = 1 \times 10^{10}\,\text{s}^{-1}$. The heating rates were 5, 10, 20 and 40°C min^{-1}. The programs of the different methods were then used; the results are shown in Tables 2a and 2b.

From Tables 2a and 2b, the results show that all programs give very good results although the differential methods give better results than the integral methods. This is expected because the approximation in the integral methods introduces some error in the calculation steps. Other papers [16–19] also emphasize the advantages of the differential methods.

Although the activation energy can be obtained from all methods, it is impossible to obtain the frequency factor value A from the multi-heating-rate methods (neither Friedman nor Ozawa methods). However, in the Friedman method, if the reaction mechanism can be obtained the

TABLE 2a

Comparison of the average E and R (standard error) values for the multi-heating-rate methods

Method	E [a] (kJ mol^{-1})	R	Deviation of E from theoretical value (%)
Friedman	120.01	1.0000	6.92×10^{-3}
Ozawa	121.74	1.0000	1.45

[a] Theoretical value of $E = 120.00\,\text{kJ mol}^{-1}$.

TABLE 2b

Comparison of E, A and R values for the single-heating-rate methods

	β (°C min^{-1})							
	Differential				Integral			
	5	10	20	40	5	10	20	40
E [a] (kJ mol^{-1})	120.01	120.02	120.03	120.06	119.55	120.69	119.56	119.96
A [b] (10^{10} s^{-1})	1.002	1.004	1.007	1.014	0.8987	1.174	0.8952	0.9888
R	1.0000	1.0000	1.0000	1.0000	1.0000	1.0000	1.0000	1.0000
Deviation of E (%)	0.00717	0.0138	0.0263	0.0501	0.375	0.575	0.366	0.320

[a] Theoretical E value is 120.00 kJ mol^{-1}. [b] Theoretical A value is 1×10^{10} s^{-1}.

frequency factor may be obtained from the intercepts, but owing to the pre-existing system error in the experimental data it is very difficult to obtain accurate frequency factors. Therefore, in this paper the Friedman and Ozawa methods are used only to check the mechanism from the activation energy values.

In the kinetic analysis of experimental data, there is an assumption that was also made in another paper [20]. The concept advanced was that the activation energies for the same mechanism for the single-heating-rate differential method and the single-heating-rate integral method should be compared. The mechanism which gives the closest agreement for E should then be selected as the preferred mechanism. Combined with the discussion above, the kinetic analysis is performed by using all the methods and the final results obtained only from the single-heating-rate methods.

Experimental results

Figures 1, 2 and 3 show the TG and DTG results with the heating curves for calcium hydroxide samples at a heating rate of 10°C min^{-1}. For commercial calcium hydroxide (Fig. 1) there is a weight loss around 100°C due to the loss of adsorbed water. For 0.1 M calcium hydroxide (Fig. 2), owing to the high solubility of calcium hydroxide (0.185 g per 100 ml water at room temperature), calcium carbonate was formed (confirmed by

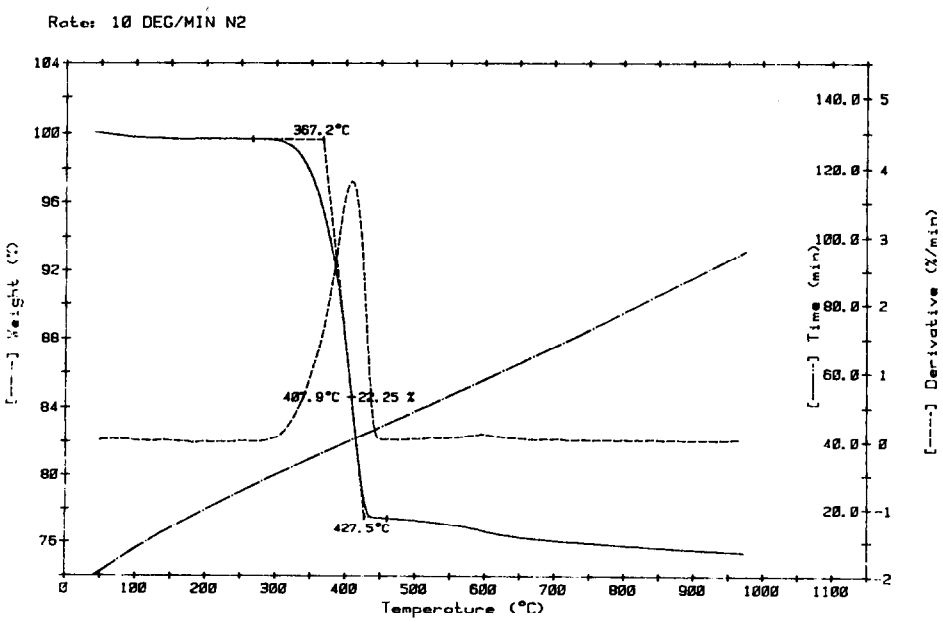

Fig. 1. The TG, DTG and heating curves for commercial calcium hydroxide at a heating rate of 10°C min^{-1}.

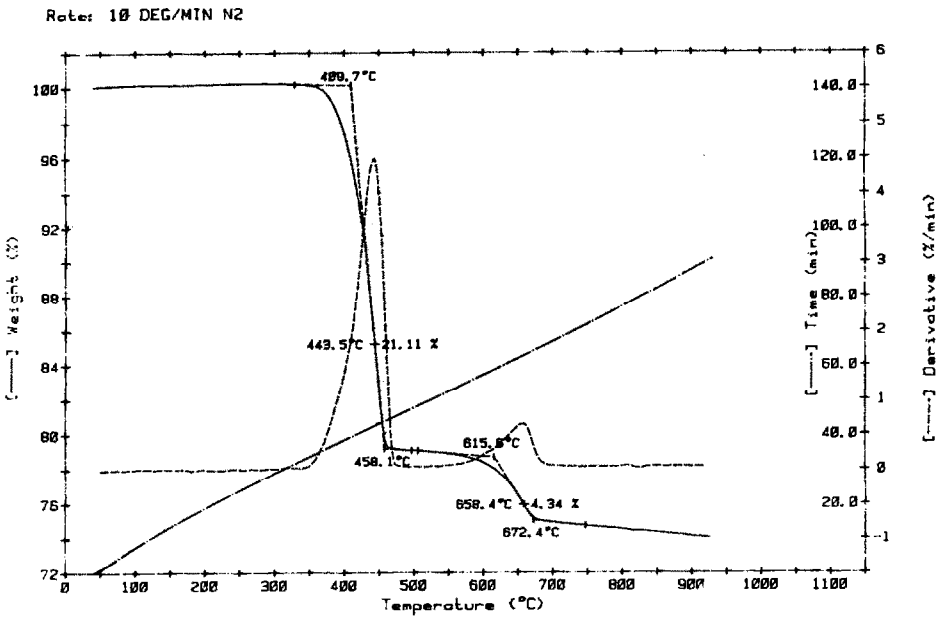

Fig. 2. The TG, DTG and heating curves for 0.1 M calcium hydroxide at a heating rate of 10°C min^{-1}.

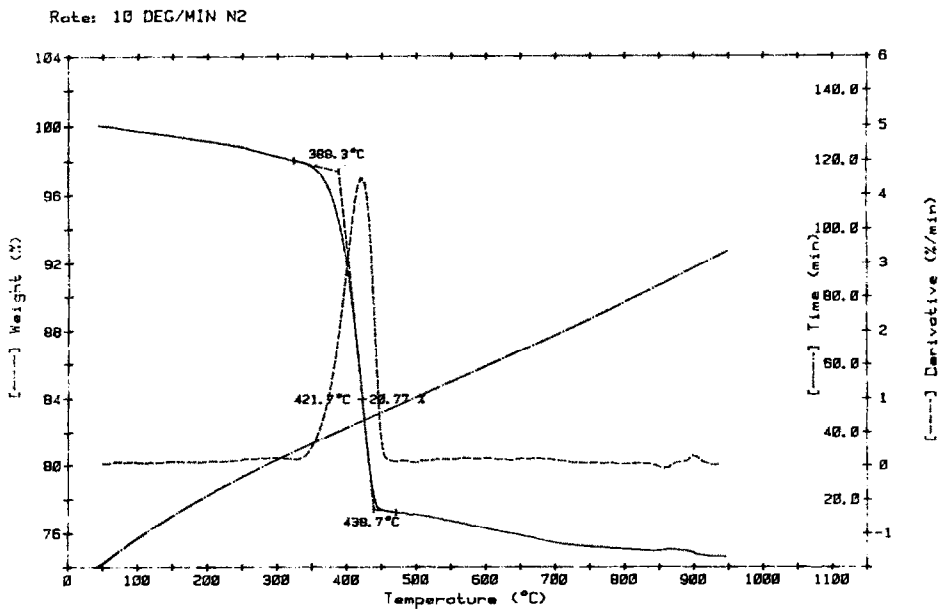

Fig. 3. The TG, DTG and heating curves for 1 M calcium hydroxide at a heating rate of 10°C min^{-1}.

TABLE 3

Surface area and peak temperature for dehydration of calcium hydroxide

Parameter	Heating rate ($°C\,min^{-1}$)	Calcium hydroxide sample		
		Commercial	0.1 M	1 M
Surface area ($m^2\,g^{-1}$)	–	16.33	3.13	18.66
Peak temperature (°C)	5	384.4	414.3	408.0
	10	407.9	443.5	421.7
	20	424.6	467.0	457.1
	30	442.9	467.8	463.8
	40	450.3	482.3	471.9

XRD) during the preparation process, which is the reason for the peak around 650°C. There is a gradual weight loss from the beginning in 1 M calcium hydroxide (Fig. 3) due to the slow release of chemisorbed and trapped water from the highly reactive calcium hydroxide.

Table 3 shows the peak temperatures and surface areas of the samples. As the heating rate increases, the peak temperature for each sample increases. However, considering the surface area with the change of peak temperature at a certain heating rate, even though the surface area of commercial calcium hydroxide ($16.33\,m^2\,g^{-1}$) is lower than that of 1 M calcium hydroxide ($18.66\,m^2\,g^{-1}$), the peak temperatures for commercial calcium hydroxide are lower than those of 1 M calcium hydroxide. The reason for this is discussed in the following section.

Figure 4 is a typical XRD pattern of calcium hydroxide and Table 4 gives a list of the half peak widths for the five highest peaks of the samples. The trend of the half peak width is

Commercial calcium hydroxide >

1 M calcium hydroxide > 0.1 M calcium hydroxide

From knowledge of XRD, the larger the value of the half peak width, the lower the crystallinity. It can be seen that the commercial calcium hydroxide has the lowest crystallinity, whereas 0.1 M calcium hydroxide has the highest crystallinity. From the scanning electron micrographs (Figs. 5 and 6), 0.1 M calcium hydroxide has the largest particle size and is well crystallized. This is also the reason for the lowest surface area of this sample. For commercial calcium hydroxide and 1 M calcium hydroxide, the micographs show that 1 M calcium hydroxide has a more uniform particle distribution but a smaller particle size. Further, 1 M calcium hydroxide has a more regular particle shape, which means better crystallinity than that of commercial calcium hydroxide. This is confirmed by the X-ray diffraction results (Table 4).

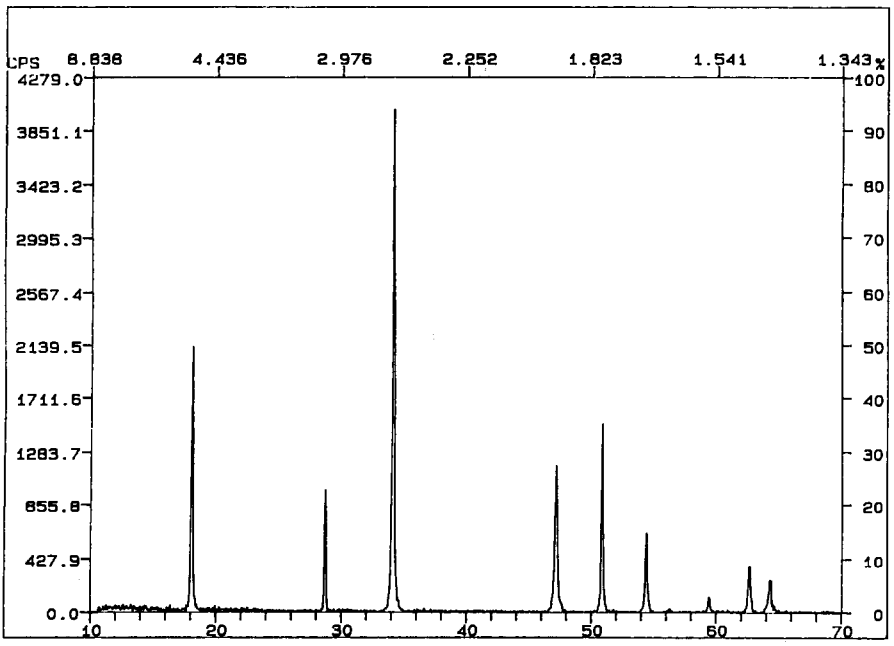

Fig. 4. Typical XRD pattern of calcium hydroxide.

Kinetic analysis

All the experimental data are calculated by using the computer programs. In order to show the process of choosing the kinetic mechanism and to obtain the kinetic parameters, the results for commercial calcium hydroxide are used as an example and the results are listed in Tables 5, 6 and 7. Tables 5 and 6 show the results calculated from the single-curve differential and integral methods respectively. From an analysis carried out by using the method advocated earlier (see section entitled Theoretical calculation), the A1.5 and F1 mechanisms are preferred, although R2 and R3 mechanisms give better regression factors and standard deviation

TABLE 4

Half peak width (ångström) of calcium hydroxide

Peak no.	2θ (deg)	Calcium hydroxide sample		
		Commercial	1 M	0.1 M
1	18.0	0.283	0.121	0.085
2	28.7	0.197	0.145	0.096
3	34.0	0.352	0.161	0.090
4	47.0	0.407	0.232	0.107
5	50.8	0.272	0.137	0.080

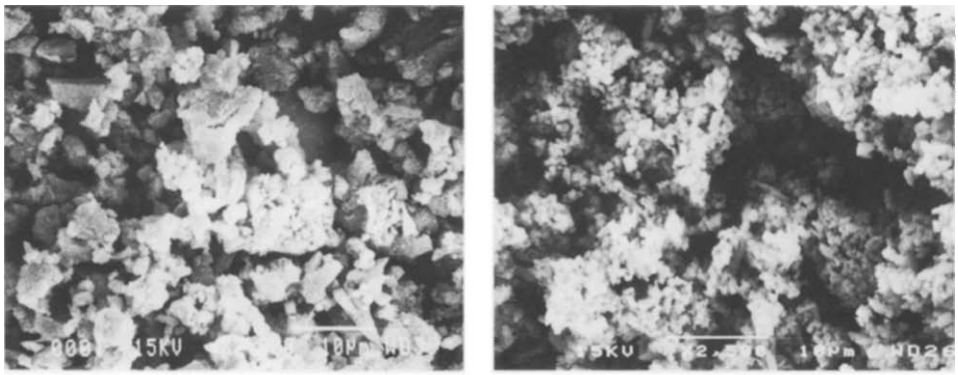

Fig. 5(a). Scanning electron micrograph of commercial calcium hydroxide at 2000×. (b). Scanning electron micrograph of 1 M calcium hydroxide at 2500×.

values. From Table 7, which gives the activation energy values from the Friedman and Ozawa methods, the A1.5 mechanism is finally chosen as the correct mechanism here because it provides closer activation energy values in all the methods. However, the regression factor values of the A1.5 mechanism are not as good as those of the F1 mechanism, but it is still the favored mechanism here; the activation energy is 96.03–107.32 kJ mol^{-1} and the value of A is 1.70×10^5 to 1.23×10^6 s^{-1}.

Figures 7 and 8 are the TG and DTG curves for commercial calcium hydroxide at a heating rate of 10°C min^{-1} (Fig. 1) overlapped by the calculated curves of differential and integral methods from the A1.5 mechanism respectively. The large shift of the peaks is because of the low regression factors. The reason for this is that the temperature of the experimental data is actually the temperature recorded by the thermocouple and is very close to the furnace temperature; this temperature will then always be lower than that of the sample due to the endothermic

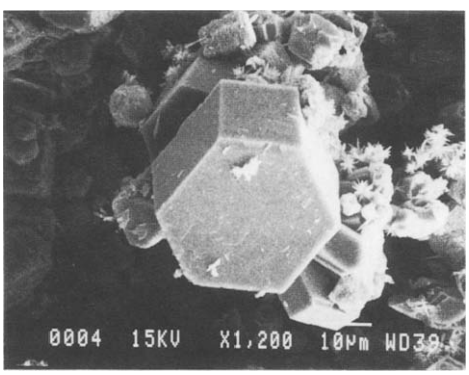

Fig. 6. Scanning electron micrograph of 0.1 M calcium hydroxide at 1200×.

TABLE 5

Results from the single-heating-rate differential method on commercial calcium hydroxide

Mechanism	Parameter	β (°C min^{-1})				
		5	10	20	30	40
A1.5	E (kJ mol^{-1})	107.32	101.46	98.90	98.72	98.55
	A (10^5 s^{-1})	12.3	3.88	3.13	3.07	3.05
	R [a]	0.9628	0.9704	0.9655	0.9705	0.9854
	S_{yx} [b]	0.2694	0.2396	0.2613	0.1924	0.1777
F1	E (kJ mol^{-1})	165.69	157.20	152.42	152.25	152.03
	A (10^{10} s^{-1})	8.98	1.18	0.52	0.45	0.37
	R [a]	0.9823	0.9863	0.9837	0.9904	0.9929
	S_{yx} [b]	0.2823	0.2500	0.2730	0.2233	0.1899
R2	E (kJ mol^{-1})	125.65	116.66	114.99	114.02	113.64
	A (10^7 s^{-1})	1.43	0.216	0.198	0.156	0.144
	R [a]	0.9971	0.9980	0.9974	0.9953	0.9935
	S_{yx} [b]	0.0854	0.0699	0.0813	0.1012	0.1362
R3	E (kJ mol^{-1})	138.99	130.18	127.46	126.89	126.44
	A (10^7 s^{-1})	13.9	2.04	1.44	1.35	1.05
	R [a]	0.9954	0.9985	0.9964	0.9986	0.9990
	S_{yx} [b]	0.1192	0.0683	0.1060	0.0809	0.0580

[a] Regression factor.
[b] Standard deviation.

decomposition reaction of the reacting sample. Further, when the reaction reaches a maximum, the temperature drop of the sample will also reach a maximum. After the reaction slows down, the temperature difference will be finally eliminated due to the higher heat exchanging rate. Therefore, for an exothermic reaction, the fitted curve should be slowly shifted to the left of the experimental curve after the reaction begins and will reach a maximum around the peak temperature; then the two curves will be merged at the end of the reaction. For an endothermic reaction, the opposite will be the case.

Based on the process and idea above, the results of 1 M calcium hydroxide and 0.1 M calcium hydroxide are calculated and analyzed. Tables 8 and 9 give the results from the single-curve methods for 1 M calcium hydroxide. Tables 10 and 11 show the results for 0.1 M calcium hydroxide. Table 12 shows the results from the multi-curve method of 0.1 M and 1 M calcium hydroxide. From Table 12 it is found that 0.1 M and 1 M calcium hydroxide have almost the same activation energies. It seems improbable from a consideration of the difference of their peak temperatures in the TG experiments, the half peak widths, in the XRD results, the scanning electron micrographs and the surface areas, but when

TABLE 6

Results from the single-curve integral method on commercial calcium hydroxide

Mechanism	Parameter	β (°C min^{-1})				
		5	10	20	30	40
A1.5	E (kJ mol^{-1})	106.68	101.08	96.42	96.26	96.03
	A (10^5 s^{-1})	10.1	3.12	1.67	1.70	1.71
	R [a]	0.9967	0.9969	0.9973	0.9978	0.9983
	S_{yx} [b]	0.0782	0.0761	0.0696	0.0605	0.0579
F1	E (kJ mol^{-1})	164.99	156.77	149.88	149.45	149.46
	A (10^{10} s^{-1})	7.32	0.947	0.275	0.207	0.209
	R [a]	0.9969	0.9971	0.9975	0.9986	0.9985
	S_{yx} [b]	0.1170	0.1139	0.1042	0.0924	0.0865
R2	E (kJ mol^{-1})	147.01	138.68	133.11	133.01	132.37
	A (10^8 s^{-1})	8.77	1.24	0.492	0.402	0.382
	R [a]	0.9937	0.9938	0.9948	0.9953	0.9955
	S_{yx} [a]	0.1485	0.1475	0.1338	0.1331	0.1322
R3	E (kJ mol^{-1})	152.56	144.24	138.28	138.01	137.61
	A (10^8 s^{-1})	18.55	2.54	0.919	0.825	0.705
	R [a]	0.9956	0.9958	0.9965	0.9970	0.9973
	S_{yx} [b]	0.1292	0.1266	0.1134	0.1087	0.1057

[a] Regression factor. [b] Standard deviation.

Tables 8 and 9 are compared with 10 and 11 and examined carefully, the difference between them is seen to be caused by the change of the reaction mechanism. When the more detailed multi-curve methods calculation is performed by decreasing the number of curves, the results show that for 1 M calcium hydroxide the average activation energy values decrease as the highest heating rate curve is removed from the calculation. For 0.1 M calcium hydroxide the opposite is true, and for 1 M calcium hydroxide the A2 mechanism is preferred. The activation energy is

TABLE 7

Activation energy values (kJ mol^{-1}) commercial calcium hydroxide from the Friedman and Ozawa methods

Method	Selected α_i					Average E (kJ mol^{-1})	Deviation
	0.1	0.3	0.5	0.7	0.9		
Friedman	119.99	125.28	119.54	108.85	112.35	115.92	7.33
Ozawa	129.35	123.77	121.40	118.29	117.64	122.37	5.22

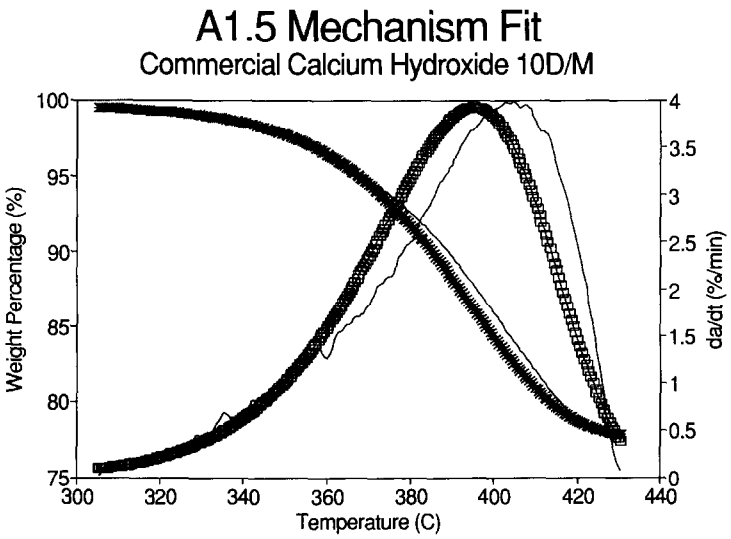

Fig. 7. The experimental and calculated (differential fit) TG and DTG curves for commercial calcium hydroxide at a heating rate of 10°C min^{-1}. Broad curves are from the calculated data.

73.98–122.48 kJ mol^{-1} and the value of A is 2.279×10^3 to 7.738×10^6 s^{-1}. For 0.1 M calcium hydroxide the A1.5 mechanism is preferred. The activation energy is 117.84–134.95 kJ mol^{-1} and the value of A is 4.041×10^6 to 2.997×10^7 s^{-1}.

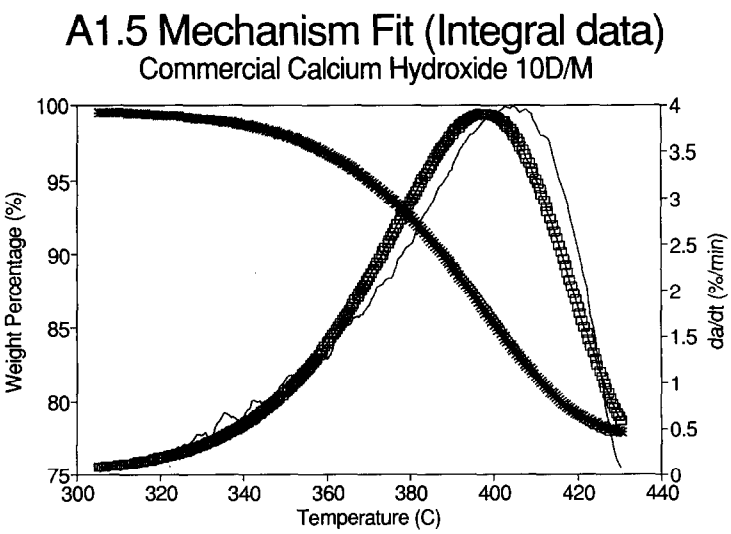

Fig. 8. The experimental and calculated (integral fit) TG and DTG curves for commercial calcium hydroxide at a heating rate of 10°C min^{-1}. Broad curves are from the calculated data.

TABLE 8

Results from the single-curve differential method on the 1 M calcium hydroxide

Mechanism	Parameter	β (°C mim^{-1})				
		5	10	20	30	40
A1.5	E (kJ mol^{-1})	164.63	146.68	136.25	115.81	106.90
	A (10^5 s^{-1})	1.92×10^5	8420	665	27.7	6.09
	R [a]	0.9835	0.9923	0.9944	0.9956	0.9964
	S_{yx} [b]	0.1860	0.1240	0.0984	0.0895	0.0793
A2	E (kJ mol^{-1})	120.25	105.90	95.67	81.27	73.98
	A (10^3 s^{-3})	5510	532	62.7	7.23	2.28
	R [a]	0.9698	0.9843	0.9866	0.9911	0.9920
	S_{yx} [b]	0.1856	0.1284	0.1076	0.0903	0.0824

[a] Regression factor. [b] Standard deviation.

Briefly, the decomposition mechanisms for commercial, 1 M and 0.1 M calcium hydroxide are A1.5, A2 and A1.5 respectively. The difference of mechanism between commercial and 1 M calcium hydroxide can explain why the peak temperatures in the TG curves of commercial calcium hydroxide is lower than those of 1 M calcium hydroxide even though commercial calcium hydroxide has a higher surface area. Further, the activation energy of 0.1 M calcium hydroxide is much larger than that of commercial calcium hydroxide.

The change of mechanisms is related to the particle size of all samples. In commercial and 0.1 M calcium hydroxide, although there is a big difference in surface area, due to the nonuniform particle size and

TABLE 9

Results from the single-curve integral method on 1 M calcium hydroxide

Mechanism	Parameter	β (°C min^{-1})				
		5	10	20	30	40
A1.5	E (kJ mol^{-1})	166.81	152.28	150.86	126.72	120.05
	A (10^6 s^{-1})	26800	2047	733.3	15.88	4.63
	R [a]	0.9984	0.9986	0.9972	0.9971	0.9968
	S_{yx} [b]	0.578	0.0536	0.0766	0.0803	0.0848
A2	E (kJ mol^{-1})	122.48	111.53	110.31	92.21	87.16
	A (10^4 s^{-1})	774	129.3	69.13	4.13	1.72
	R [a]	0.9983	0.9986	0.9970	0.9968	0.9965
	S_{yx} [b]	0.0435	0.0404	0.0577	0.0607	0.0641

[a] Regression factor. [b] Standard deviation.

TABLE 10

Results from the single-curve differential on 0.1 M calcium hydroxide

Mechanism	Parameter	β (°C min^{-1})				
		5	10	20	30	40
A1.5	E (kJ mol^{-1})	128.35	137.33	126.49	117.84	119.47
	A (10^6 s^{-1})	24.9	85.1	10.4	3.57	4.29
	R [a]	0.9446	0.9604	0.9861	0.9875	0.9832
	S_{yx} [b]	0.3168	0.2810	0.1714	0.1567	0.1837
A2	E (kJ mol^{-1})	93.12	100.83	92.53	84.84	86.53
	A (10^4 s^{-1})	3.70	13.3	3.07	1.24	1.66
	R [a]	0.9026	0.9325	0.9756	0.9759	0.9694
	S_{yx} [b]	0.3156	0.2756	0.1679	0.1584	0.1816

[a] Regression factor. [b] Standard deviation.

TABLE 11

Results from the single-curve integral method on the 0.1 M calcium hydroxide

Mechanism	Parameter	β (°C min^{-1})				
		5	10	20	30	40
A1.5	E (kJ mol^{-1})	130.28	134.95	124.44	120.57	120.12
	A (10^6 s^{-1})	30.0	47.7	6.51	4.92	4.04
	R [a]	0.9954	0.9963	0.9986	0.9982	0.9984
	S_{yx} [b]	0.0892	0.0822	0.0536	0.0610	0.0563
A2	E (kJ mol^{-1})	95.09	98.48	90.51	87.61	87.21
	A (10^4 s^{-1})	4.45	7.41	1.91	1.69	1.55
	R [a]	0.9951	0.9961	0.9985	0.9980	0.9983
	S_{yx} [b]	0.0670	0.0617	0.0403	0.0460	0.0424

[a] Regression factor. [b] Standard deviation.

TABLE 12

Activation energies of 0.1 M and 1 M calcium hydroxide from the multi-curve methods

Calcium hydroxide sample	Friedman		Ozawa	
	Average E (kJ mol^{-1})	Standard deviation	Average E (kJ mol^{-1})	Standard deviation
0.1 M	101.78	11.98	118.36	3.24
1 M	99.49	15.95	118.88	9.03

impurity (referred to as the calcium carbonate) in the 0.1 M sample, their mechanisms are different from that of 1 M calcium hydroxide, which has a more uniform particle size. However, all samples do fall in the same mechanism group, namely the Avrami–Erofeev. The physical meaning of this mechanism [21] is that impingement and coalescence of developed nuclei occurs with ingestion of undeveloped nucleation sites. The integral equation form of the Avrami–Erofeev mechanisms is

$$G(\alpha) = [-\ln(1-\alpha)]^{1/n}$$

where $n = 1.5$ and 2 for the A1.5 and A2 mechanisms respectively. According to the deduction process of this equation, $n = \lambda + \beta$, where β is the number of steps involved in nucleus formation and λ is the number of dimensions in which the nuclei grow. Most frequently, β equals 0, which corresponds to instantaneous nucleation. From the results of the kinetic analysis, owing to the small particle size in 1 M calcium hydroxide, a two-dimensional nuclei growth is seen which also means in crystals that the reaction occurs from the edge planes but not from the hexagonal planes. This is also confirmed in another study [22]. For commercial and 0.1 M calcium hydroxide, owing to the nonuniform particle distribution and impurity in 0.1 M calcium hydroxide, one plane of the crystal dominates the reaction, and another plane is also favored but at a lower reaction rate. Therefore, a change of particle size and distribution changes the reaction mechanism. The trends observed from this research are that the more uniform the particle size, the higher the reaction dimensions and the larger the particle, the lower the reaction dimensions.

CONCLUSIONS

The most probable kinetic mechanism functions are determined as A1.5 for commercial calcium hydroxide and 0.1 M calcium hydroxide and A2 for 1 M calcium hydroxide in the heating rate ranges 5–40°C min^{-1}. For commercial calcium hydroxide, the activation energy is 96.03–107.32 kJ mol^{-1} and A equals 1.70×10^5 to 1.23×10^6 s^{-1}. For 0.1 M calcium hydroxide, the activation energy is 117.84–134.95 kJ mol^{-1} and A equals 4.041×10^6 to 2.997×10^7 s^{-1}. For 1 M calcium hydroxide, the activation energy is 73.98–122.48 kJ mol^{-1} and A is 2.279×10^3 to 7.738×10^6 s^{-1}.

The variation in reaction mechanism is related to the particle size and the distribution of size. The more uniform the particle size, the higher the reaction dimensions. The larger the particle size, the lower the reaction dimensions. The use of the four kinetic analysis methods are more practical and can differentiate the reaction mechanism more easily than hitherto.

ACKNOWLEDGMENTS

The authors thank Ewa Skrzypczak-Jankun and Pannee Burckel for their help in the XRD and SEM experiments.

REFERENCES

1 H. Le Chatelier, C.R. Acad. Sci., 102 (1886) 1243.
2 J. Johnston, Z. Phys. Chem., 62 (1908) 330.
3 D. Dragert, Doctoral Dissertation, Berlin, 1914.
4 S. Tamaru and K. Shiomi, Z. Phys. Chem., Abt. A, 161 (1932) 421.
5 F.M. Lea and Desch, Chemistry of Cement and Concrete, 3rd edn., Arnold, London, 1970, p. 30.
6 P.E. Halstead and A.E. Moore, J. Chem. Soc. (1957) 3873.
7 J.M. Crido and J. Morales, J. Therm. Anal. 10 (1976) 103.
8 J.N. Mayock and J. Skalny, Thermochim. Acta, 8 (1974) 167.
9 D. Dollimore and P. Spooner, J. Appl. Chem. Biotechnol., 24 (1974) 35.
10 A.W. Coats and J.P. Redfern, Nature, 201 (1964) 68.
11 J.R. MacCallum and J. Tanner, Eur. Polym. J., 6 (1970) 1033.
12 P.M. Madhusudanan, Thermochim. Acta, 97 (1986) 189.
13 H. Friedman, J. Polym. Sci., 50 (1965) 183.
14 T. Ozawa, Bull. Chem. Soc. Jpn., 38 (1965) 1881.
15 D. Chen, X. Gao and D. Dollimore, Analyt. Instrum., 20 (1992) 137.
16 J.H. Flynn, J. Therm. Anal., 27 (1983) 95.
17 T. Ozawa, J. Therm. Anal., 31 (1986) 547; Thermochim. Acta, 100 (1986) 109.
18 J. Elder, J. Therm. Anal., 36 (1990) 1077.
19 J.H. Flynn, J. Therm. Anal., 37 (1991) 293.
20 X. Gao, D. Chen and D. Dollimore, in preparation.
21 M.E. Brown, D. Dollimore and A.K. Galwey, in C.H. Bamford and C.F.H. Tipper (Eds.), Comprehensive Chemical Kinetics, Elsevier, Amsterdam, Vol. 22, 1985, 340 pp.
22 J.I. Bhatty, K.J. Reid, D. Dollimore, G.A. Gamlen, R.J. Mangabhai, P.F. Rogers and T.H. Shah, Compositional analysis by thermogravimetry, Am. Soc. Test. Mater., Spec. Tech. Publ., 997 (1988) 204.